

# Empirical Capacitive Deionization ANN Nonparametric Modeling for Desalination Purpose

Adel El Shahat

**Abstract**— This paper proposes Capacitive Deionization (CDI) Operational Conditions Nonparametric Modeling for desalination purposes. CDI technique is advantageous due to its low energy consumption, low environmental pollution, and low fouling potential. The objective of this paper is to model the investigation of different operational conditions (Total Dissolved Solids (TDS) concentration, temperature, flow rate) effect on the CDI electrosorption efficiency and energy consumption. The modeling based on real experimental data with Laboratory scale experiments were conducted by using a commercial CDI with activated carbon electrodes developed by Aque EWP [1], as a training data and express them as algebraic functions to connect between various operational characteristics. This is done by developing four models with the aid of Artificial Neural Network (ANN). First one to express electrosorptive performance of CDI at different solution temperatures with Temperature and Time as inputs and TDS as output. Second one for Efficiency as output with Temperature, Time and TDS as inputs. Third one to illustrate effect of flow rate on electrosorption efficiency and energy consumption with Flow Rate and Time as inputs and TDS as output. Forth one for Energy Consumption as output and Operational Flow Rate, Time and TDS as inputs. All characteristics are well depicted in the form of 3D figures as the training data for ANN models to show the validity of the proposed technique in interpolations and estimations. ANN technique models are adopted for various characteristics estimation process and generation of functions for these experimental data due to its advantages. ANN models are created with suitable numbers of layers and neurons, which trained, simulated, checked, verified and their algebraic equations are concluded accurately with excellent regression constants.

**Index Terms**— Capacitive Deionization (CDI), modeling, neural network, and estimation.

## I INTRODUCTION

The clean water is one of the key technological, social, and economical challenges of the 21st century. It is acknowledged as a basic human right by the United Nations [5]. Currently techniques such as reversible osmosis, electro dialysis or distillation are applied to desalinate salty water. Capacitive Deionization (CDI) has emerged over the years as a robust, energy efficient, and cost effective technology for desalination of water with a low or moderate salt content [1]-[3], and as promising energy efficient method. A simple operational principle is shown in Fig. 1. The system consists of a fluidic in- and outlet with channel in between. Within the channel two desalination electrodes are situated which in our case are situated within the same plane. Salt water enters the channel and a potential is applied across the electrodes. The cations and anions will be attracted to oppositely charged electrodes and are stored in the electrical double layer. After the electrodes are saturated, the system is regenerated [2], [4]. This technique is specifically interesting for portable desalination units.

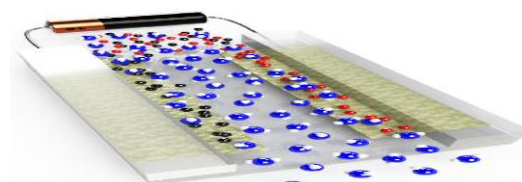


Figure 1 Capacitive deionization. A potential is applied across two electrodes. Ions are attracted to the oppositely charged electrode. Fresh water exits the system. After the electrodes are saturated, the system is regenerated.

CDI operates at a relatively low electrical voltage for the removal of ions and it doesn't produce any secondary regeneration wastes [4], [6]. In addition, CDI doesn't require pressure driven membranes or high pressure pumps so that it avoids the scaling problems that always occur with conventional membrane based technologies for desalination [7], [8]. Regeneration of electrodes is then required by applying a reverse potential to the electrodes to get rid of the adsorbed ions into the waste stream [9]. Electrosorptive performance with modified activated carbon cloth as CDI electrodes was also investigated [10]. Some papers paid attention on the effect of operational conditions to CDI, efficiency and energy consumption [11] – [14]. Some researches depend on Artificial Neural Network too for modeling desalination techniques [15]. Response surface methodology (RSM) and

• Adel El Shahat with Department of Electrical and Computer Engineering at University of Illinois, Chicago (UIC) as a Visiting Assistant Professor, and Assistant Professor in Engineering Science Department, Faculty of Petroleum and Mining Engineering, Suez University, Egypt.

artificial neural network (ANN) have been used to develop predictive models for simulation and optimization of reverse osmosis (RO) desalination process [16]. A solar powered membrane distillation system has been used for developing an optimizing control strategy using ANN model of the system based on experimental data under various operating conditions [17]. Comparative energy consumption analysis study of capacitive deionization are adopted [18]. A nonlinear inverse model control strategy based on neural network is proposed for desalination plant to handle complex and nonlinear process relationships [19]. Many benefits drawn from previous works were applied to this work. This work addresses the nonparametric modeling of Capacitive Deionization (CDI) Operational Conditions. This model investigates the effects operational conditions like: Total Dissolved Solids (TDS) concentration, temperature, and flow rate on the CDI electrosorption efficiency and energy consumption. The modeling here based on several electrosorption experiments were conducted by using a commercial CDI technology AQUA EWP at different flow rates, feed solution TDS concentrations and solution temperatures as shown in [1]. This real experimental data is used as a training data to be expressed as algebraic functions to connect between various operational characteristics. Four ANN models are developed to predict and estimate the performance within the range of the training data for the measured and unmeasured values. 1<sup>st</sup> model for electrosorptive performance of CDI at different solution temperatures which take Temperature and Time as inputs and TDS as output. 2<sup>nd</sup> model for Efficiency as output with Temperature, Time and TDS as inputs. 3<sup>rd</sup> model for effect of flow rate on electrosorption efficiency and energy consumption with Flow Rate and Time as inputs and TDS as output. 4<sup>th</sup> model for Energy Consumption as output and Operational Flow Rate, Time and TDS as inputs. All characteristics are well depicted in the form of 3D figures as the training data for ANN models. ANN technique models are adopted for various characteristics estimation process and generation of functions for these experimental data due to its advantages. ANN models with Back - Propagation (BP) technique are created with suitable numbers of layers and neurons, which trained, simulated, checked, verified and their algebraic equations are concluded accurately with excellent regression constants. The ANN models' algebraic equations are deduced for use directly. These models are validated in the means of comparisons between real data and simulated corresponding data from ANN model with excellent acceptable error between targets and outputs.

## II THE COMMERCIAL CDI PILOT PLANT [1]

The commercial CDI unit used in this research [1], was developed by AQUA EWP, USA. Fig. 2 shows a schematic diagram of the used CDI unit. As shown in it, the influent water is pumped from a storage tank through a pre-filter and afterwards passes over a flow weir to measure the influent flow to two carbon electrode cells connected in series. The electrodes within the cell are chargeable by applied DC potential in the range of 1 to 1.5 VDC. The whole operational

cycle of the CDI takes 2.5 minutes. The cycle consists of two main steps, the regeneration mode step and the purification mode step [1]. The regeneration step commences with 30 seconds when the effluent solenoid valve (SV1) and the influent solenoid valve (SV0) are closed and the supplied power is off, followed by another 30 seconds when the effluent waste solenoid valve (SV2) and the influent solenoid valve (SV0) are opened and the power is turned on with opposite polarity of 1.5 VDC. After 60 seconds the regeneration step finished. The purification step is started immediately following this and it takes 90 seconds to purify the feed solution. Here the influent solenoid valve (SV0) and the effluent solenoid valve (SV1) are opened. The CDI contains a critical acid cleaning tank for the cleaning of the electrodes when the purification doesn't meet the standards. A heater was supplied to maintain the required temperature for the feed solution [1].

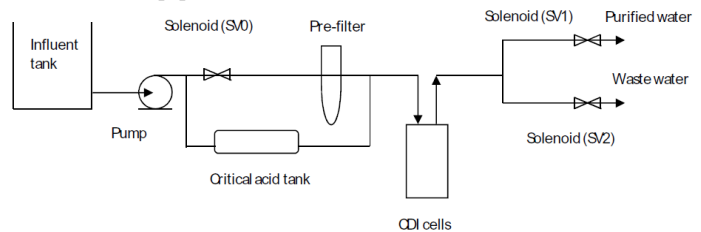


Figure 2 CDI schematic diagram

Fig. 3. Shows a schematic diagram of the CDI cells construction. The electrodes are mainly composed of activated carbon with an organic binder. Each cell contains a mass of 1354 grams of activated carbon. The electrodes within the cell consist of a conductive surface sandwiched between layers of activated carbon. A nonconductive spacer material separates the plates from each other. These electrodes are connected to two sides of DC power supply by using connecting leads [1].

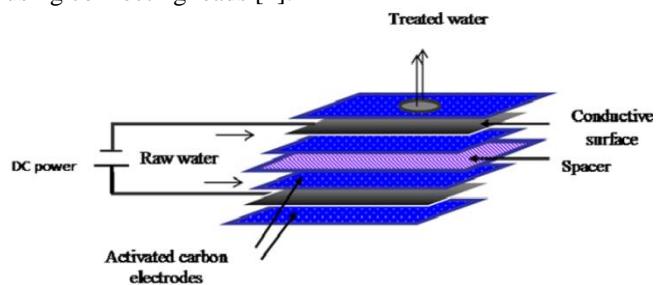


Figure 3 CDI construction schematic diagram

## III Experimental Data

A series of laboratory experiments were conducted to investigate the effect of operational conditions (TDS concentration, flow rate, temperature) on the CDI electrosorption efficiency and energy consumption [1].

### A Electrosorptive performance of CDI at different temp.s

Fig. 4. Shows the purified stream TDS concentration of the CDI unit at different temperatures. It is shown that puri-

fied stream TDS concentration increases gradually by increasing solution temperature. These results in [1], are consistent with the results reported by Xu et al. [7] in treating brackish produced water from a natural gas operation site.

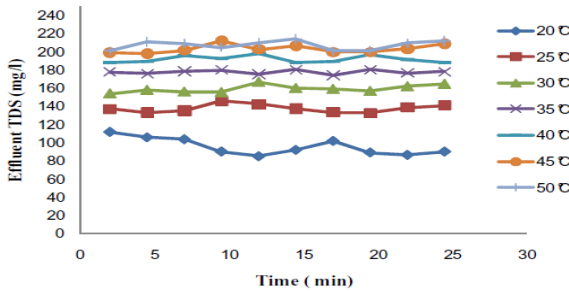


Figure 4 TDS at different feed solution temperatures [1], [7]

Fig. 5. Shows the relationship of electrosorption removal efficiency and solution temperature [1]. It can be noticed that the electrosorption removal efficiency is inversely proportional to solution temperature. As a result, higher electrosorption removal efficiency at low temperature may be caused by the transition from hydrophobic to hydrophilic transitions on the surface of the activated carbon [20].

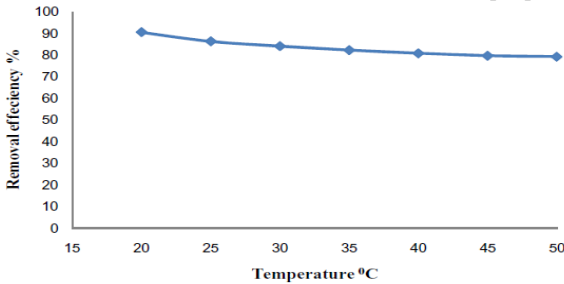


Figure 5 Removal efficiency as a function of solution temperature [1], [20]

It is notified from figure 5, the removal efficiency is changed from 90% to 80% when the temperature changed from 20 to 50 degree. The change in the removal efficiency is not so significant comparing with the change of the temperature as one of the advantages of this experimental apparatus as shown from these measured results.

**B Effect of flow rate on elec. efficiency & energy consum.**

Fig. 6. Depicts the variation of the purified stream TDS concentration with different flow rates [1]. It is shown that the TDS concentration increases by increasing the flow rate. These results are consistent with the results reported by Li et al. [21].

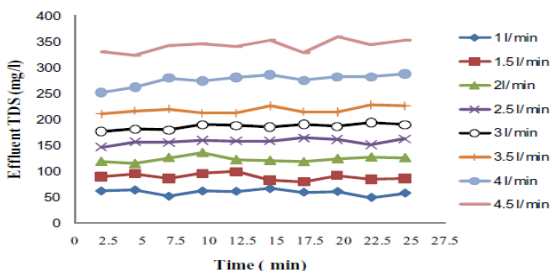


Figure 6 Purified stream TDS at different flow rates [1], [21]

Fig. 7 shows the effect of different operational flow rates on the energy consumption. It is seen that as the flow rate increases the energy consumption decreases [1], [21].

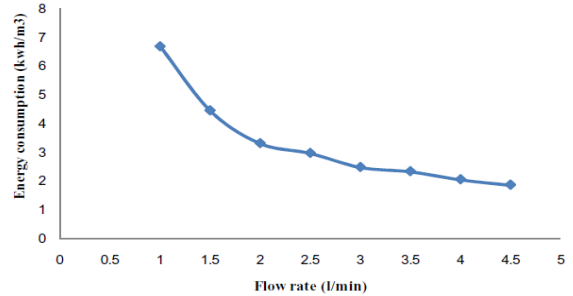


Figure 7 Effect of operational flow rate on energy consumption [1], [21]

The previous figures are used as training or learning data for the ANN models as shown later.

**IV ARTIFICIAL NEURAL NETWORK MODELING**

Using the Artificial Neural Network (ANN), with back-probagation technique [22]-[29] to implement four models; First one to express electrosorptive performance of CDI at different solution temperatures with Temperature and Time as inputs and TDS as output. Second one for Efficiency as output with Temperature, Time and TDS as inputs. Third one to illustrate effect of flow rate on electrosorption efficiency and energy consumption with Flow Rate and Time as inputs and TDS as output. Forth one for Energy Consumption as output and Operational Flow Rate, Time and TDS as inputs, to help in modeling, parameters and characteristics estimation. This is done to make benefits from the ability of neural network of interpolation between points and also curves. Finally, the algebraic equations are deduced to use it without training the neural unit in each time.

**A CDI Temperatures Electrosorptive ANN Model**

This model' inputs are the Temperature and Time and TDS as output as shown in Fig. 8.



Figure 8 A schematic diagram of 1st ANN model

The model algebraic equation is deduced as the following:

$$\text{Temperature}_n = (\text{Temperature} - 35) / (10.0722) \quad (1)$$

$$\text{Time}_n = (\text{Time} - 13.5288) / (7.3753) \quad (2)$$

The previous Equations present the normalized inputs (subscript n denotes normalized variable) for the ANN model and the following equations lead to the required derived output equation.

$$\mathbf{E} = \begin{bmatrix} E1 \\ E2 \\ E3 \\ E4 \\ E5 \\ E6 \\ E7 \\ E8 \\ E9 \\ E10 \\ E11 \\ E12 \\ E13 \\ E14 \\ E15 \\ E16 \\ E17 \\ E18 \\ E19 \end{bmatrix} = \begin{bmatrix} -5.1074 & 5.2126 \\ 8.4632 & 3.4806 \\ -11.8202 & 5.1140 \\ -3.6100 & -9.1978 \\ -37.3702 & 20.2396 \\ -22.5872 & -30.6987 \\ -8.5233 & -6.4870 \\ -1.6723 & -12.6005 \\ 8.8656 & 6.9946 \\ 1.1346 & -6.4739 \\ -31.1204 & -21.7481 \\ -5.2008 & -3.6752 \\ 16.5069 & -3.5788 \\ 40.9043 & -57.0242 \\ -1.5423 & 5.9485 \\ -2.5752 & -1.4811 \\ 12.7141 & -20.6490 \\ -15.9212 & -23.9918 \\ -17.1242 & -21.5390 \end{bmatrix} \begin{bmatrix} \text{Temperature}_n \\ \text{Time}_n \end{bmatrix} + \begin{bmatrix} -11.7305 \\ -13.8384 \\ -10.0773 \\ 9.4148 \\ -18.8371 \\ 27.6660 \\ 0.8668 \\ 2.9976 \\ -0.9320 \\ 1.8362 \\ -14.9842 \\ -1.2455 \\ -2.7077 \\ -49.1781 \\ 9.2137 \\ 0.0441 \\ -24.8413 \\ -37.9330 \\ -52.3686 \end{bmatrix} \quad (3)$$

$$F_{1,19} = 1 / (1 + \exp(-E_{1,19})) \quad (4)$$

$$\begin{aligned}
 TDS_n = & 0.4576 F1 + 0.3075 F2 + 0.1498 F3 + 0.5261 F4 + \\
 & 0.2253 F5 - 0.3082 F6 + 11.5199 F7 + 0.6728 F8 + 9.3616 F9 \\
 & - 1.1421 F10 + 1.8441 F11 - 3.3387 F12 - 0.2748 F13 \\
 & - 0.4592 F14 + 1.8162 F15 - 2.2549 F16 \\
 & - 0.1481 F17 - 0.4842 F18 - 0.5150 F19 - 10.0259
 \end{aligned} \quad (5)$$

The un- normalized output

$$TDS = 38.2848 TDS_n + 168.0582 \quad (6)$$

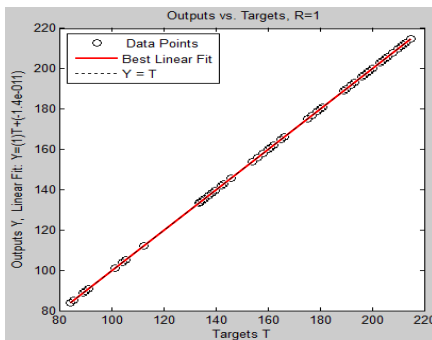


Figure 9 Output VS Target for 1<sup>st</sup> Model

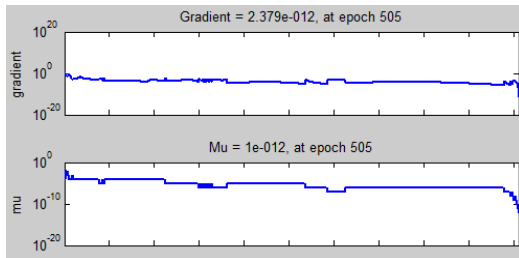


Figure 10 Training state and error for 1<sup>st</sup> Model

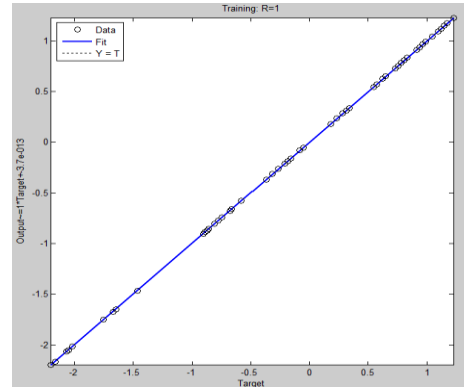


Figure 11 Regression for 1<sup>st</sup> Model = 1

### B Electrosorption Removal Efficiency ANN Model

This model' inputs are Temperature, Time and TDS and the output is Electrosorption Efficiency as shown in Fig. 12.



Figure 12 A schematic diagram of 2<sup>nd</sup> ANN model

The model algebraic equation is deduced as the following with using the previous normalized Eq.s for inputs.

$$\mathbf{E} = \begin{bmatrix} E1 \\ E2 \\ E3 \end{bmatrix} = \begin{bmatrix} 0.0713 & 0.0094 & -26.0098 \\ 125.9409 & -85.6763 & -235.0903 \\ -1.1231 & -0.0065 & -0.0494 \end{bmatrix} \begin{bmatrix} \text{Temperature}_n \\ \text{Time}_n \\ \text{TDS}_n \end{bmatrix} + \begin{bmatrix} -39.8512 \\ 31.6599 \\ -0.9894 \end{bmatrix} \quad (7)$$

$$F_{1,2,3} = 1 / (1 + \exp(-E_{1,2,3})) \quad (8)$$

$$\text{Efficiency}_n = 3.2296 F1 + -0.0157 F2 + 3.7335 F3 + -1.2829 \quad (9)$$

The un- normalized output

$$\text{Efficiency} = 0.0366 \text{Efficiency}_n + 0.8386 \quad (10)$$

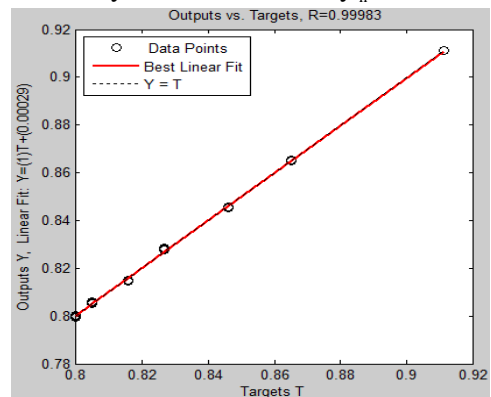


Figure 13 Output VS Target for 2<sup>nd</sup> Model

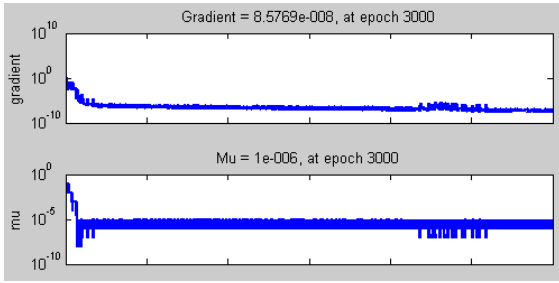


Figure 14 Training state and error for 2<sup>nd</sup> Model

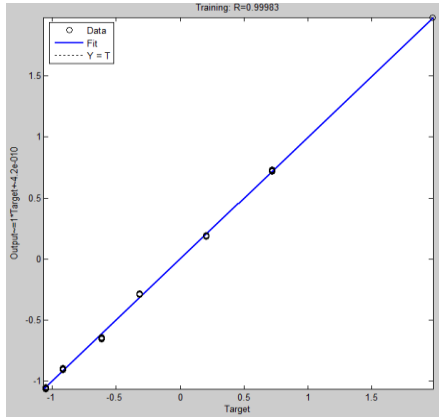


Figure 15 Regression for 2<sup>nd</sup> Model = 0.99983

The data is well depicted in the following 3D figures for the inputs and targets (outputs) of the previous two models (1<sup>st</sup> and 2<sup>nd</sup>) to adequate with the function of ANN technique and cover all data as mapping surface.

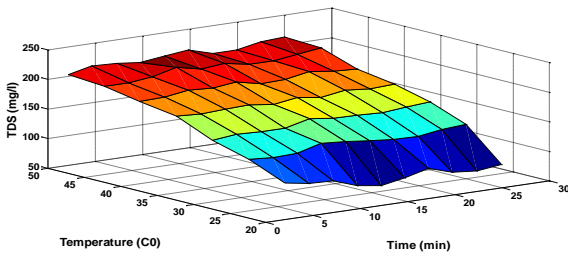


Figure 16 3D relation for TDS, Temperature with time

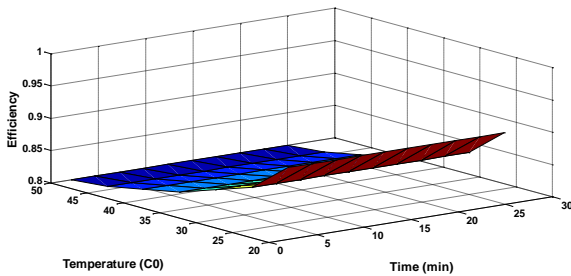


Figure 17 3D relation for Efficiency, Temperature with time

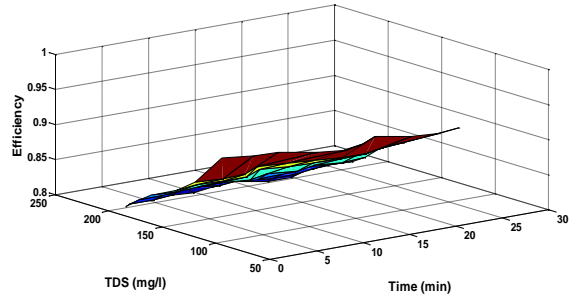


Figure 18 3D relation for Efficiency, TDS with time

### C CDI Different flow rate Electroosrptive Perf. ANN Model

This model' inputs are Flow Rate and Time as inputs and TDS as output as shown in Fig. 19.



Figure 19 A schematic diagram of 3<sup>rd</sup> ANN model

The model algebraic equation is deduced as the following:

$$FlowRate_n = (FlowRate - 2.75) / (1.1529) \quad (11)$$

$$Time_n = (Time - 13.2811) / (7.2835) \quad (12)$$

Eq. s (11), (12) present normalized inputs.

$$E = \begin{bmatrix} E1 \\ E2 \\ E3 \\ E4 \\ E5 \\ E6 \\ E7 \\ E8 \\ E9 \\ E10 \\ E11 \\ E12 \\ E13 \\ E14 \\ E15 \\ E16 \\ E17 \\ E18 \\ E19 \end{bmatrix} = \begin{bmatrix} 6.2694 & -1.4885 \\ 9.6058 & -4.8209 \\ 1.4545 & 3.6485 \\ -1.8948 & 11.9205 \\ -6.7441 & -2.9265 \\ -19.9672 & -0.0504 \\ 39.4286 & 13.1414 \\ 3.3973 & 4.5344 \\ 4.2165 & 3.4837 \\ 11.3965 & -0.1393 \\ -24.4477 & -0.1350 \\ 341.6156 & 270.1071 \\ 259.7941 & -74.7493 \\ -0.7514 & 8.5214 \\ 19.8465 & 0.0544 \\ 7.3834 & 8.1317 \\ -3.6891 & -11.2186 \\ 4.3413 & -1.6329 \\ 4.3580 & -1.6373 \end{bmatrix} \begin{bmatrix} Flow\_Rate_n \\ Time_n \end{bmatrix} + \begin{bmatrix} -19.1709 \\ 11.9169 \\ -5.8240 \\ -11.2623 \\ 8.0410 \\ -14.2694 \\ -40.4584 \\ 2.5968 \\ -2.1304 \\ 0.0006 \\ 2.0274 \\ 119.4340 \\ -181.5033 \\ 4.6215 \\ 14.1624 \\ 12.5202 \\ -18.7938 \\ -6.4582 \\ -6.4798 \end{bmatrix} \quad (13)$$

$$F_{1:19} = 1 / (1 + \exp(-E_{1:19})) \quad (14)$$

$$TDS_n = 1109.9 F1 - 0.2 F2 + 1.3 F3 + 0.4 F4 - F5 + 618.7 F6 - 0.5 F7 + 0.4 F8 + 0.7 F9 - 6.6 F10 - 5.3 F11 + 0.2 F12 - 0.4 F13 + 0.2 F14 + 619.2 F15 + 0.4 F16 + -0.4 F17 + 312 F18 - 312 F19 - 613.1402 \tag{15}$$

The un- normalized output

$$TDS = 90.3743 TDS_n + 181.3325 \tag{16}$$

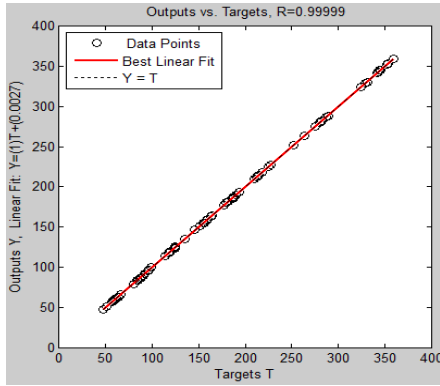


Figure 20 Output VS Target for 3<sup>rd</sup> Model

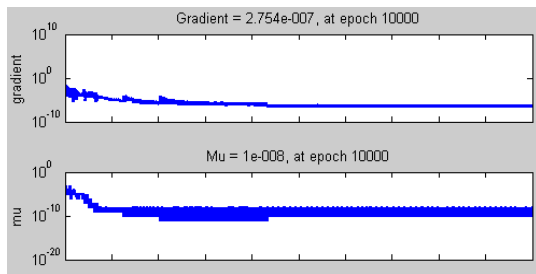


Figure 21 Training state and error for 3<sup>rd</sup> Model

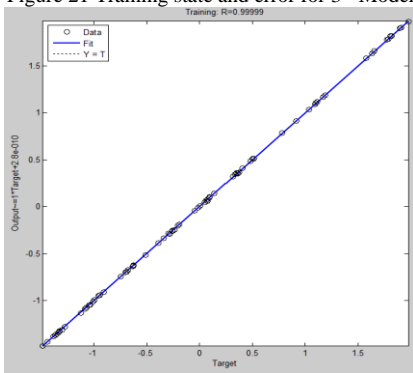


Figure 22 Regression for 3<sup>rd</sup> Model = 0.99999

### D Energy Consumption ANN Model

This model' inputs are Operational Flow Rate, Time and TDS; Energy Consumption is the output as shown in Fig. 23.



Figure 23 A schematic diagram of 4<sup>th</sup> ANN model

The model algebraic equation is deduced as the following with using the previous normalized Eq.s for inputs.

$$E = \begin{bmatrix} E1 \\ E2 \\ E3 \end{bmatrix} = \begin{bmatrix} -5.6641 & -0.1956 & 3.0769 \\ -58.0280 & -0.0159 & 0.1877 \\ 7.5388 & 0.4935 & -7.0334 \end{bmatrix} \begin{bmatrix} \text{Flow\_Rate}_n \\ \text{Time}_n \\ \text{TDS}_n \end{bmatrix} + \begin{bmatrix} 0.1002 \\ -63.5309 \\ -1.3085 \end{bmatrix} \tag{17}$$

$$F_{1,2,3} = 1 / (1 + \exp(-E_{1,2,3})) \tag{18}$$

$$\text{Energy\_Consumption}_n = 1.1306 F1 + 2.127 F2 + 0.3765 F3 - 1.0036 \tag{19}$$

The un- normalized output

$$\text{Energy\_Consumption} = 1.5219 \text{Energy\_Consumption}_n + 3.26 \tag{20}$$

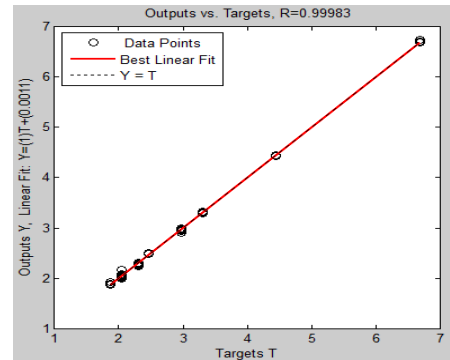


Figure 24 Output VS Target for 4<sup>th</sup> Model

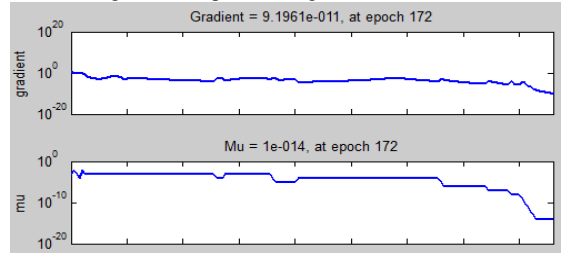


Figure 25 Training state and error for 4<sup>th</sup> Model

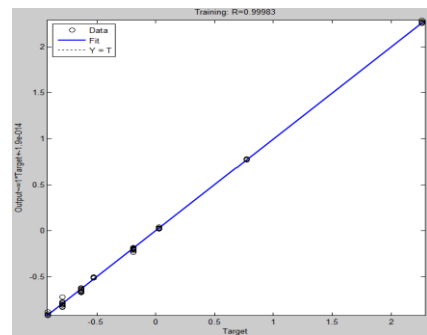


Figure 26 Regression for 4<sup>th</sup> Model = 0.9998

The data is well depicted in the following 3D figures for the inputs and targets (outputs) of the previous two (3<sup>rd</sup>, and 4<sup>th</sup>) models to adequate with the function of ANN technique and cover all data as mapping surface.

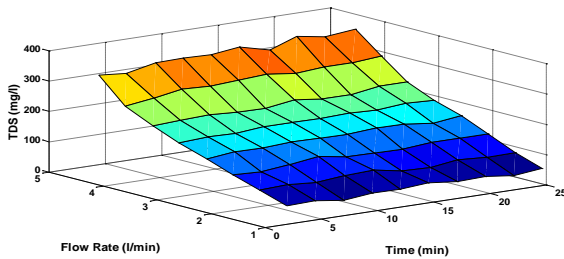


Figure 27 3D relation for TDS, Flow Rate with time

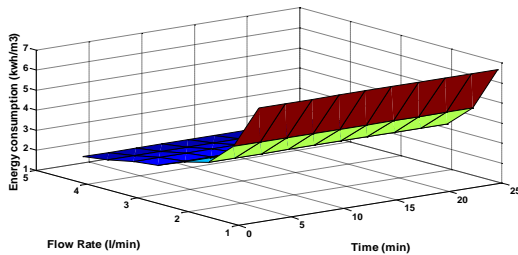


Figure 28 3D relation for Energy Consumption, Flow Rate with time

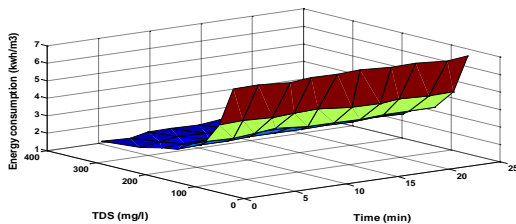


Figure 29 3D relation for Energy Consumption, TDS with time

## V CONCLUSION

This paper gives a point of view for CDI technology as a novel electrosorption process for water desalination. CDI has many advantages due to its low energy consumption, low environmental pollution, and low fouling potential. This work addresses the nonparametric modeling of Capacitive Deionization (CDI) Operational Conditions. The modeling here based on several electrosorption experiments were conducted by using a commercial CDI technology AQUA EWP at different flow rates, feed solution TDS concentrations and solution temperatures as shown in [1]. Four ANN models are efficiently developed to predict and estimate the performance within the range of training data for the measured and unmeasured values. 1<sup>st</sup> model takes Temperature and Time as inputs and TDS as output. 2<sup>nd</sup> model for Efficiency as output with Temperature, Time and TDS as inputs. 3<sup>rd</sup> model takes Flow Rate and Time as inputs and TDS as output. 4<sup>th</sup> model for Energy Consumption as output and Operational Flow Rate, Time and TDS as inputs. All characteristics are well depicted in the form of 3D figures. ANN models with Back - Propagation (BP) technique are created with suitable numbers of layers and neurons. The ANN models' algebraic equations are deduced for directly usage. The results obtained are sufficiently accurate to apply the models involving less computational efforts. These models are checked and verified by comparing actual and predicted ANN values, with a good errors values and excellent regres-

sion factors between 0.99983 to 1 imply accuracy. Artificial neural networks (ANNs) can handle complex and nonlinear process relationships, and are robust to noisy data. Also, the neural networks are trained for nearly 70% of these training data extracted and then checked for the rest 30% with the 70%, i.e. for the whole 100% range in the form of comparisons. The data used not only the dotted one but also some from in between the shown points for more visibility. ANN is also used for all the whole ranges and in between curves (which we do not know) like the 3D figures shown for all parameters and characteristics.

## REFERENCES

- [1] Mohamed Mossad and Linda Zou, "Effects of operational conditions on the electrosorption efficiencies of Capacitive deionization", Chemeca 2011, Engineering a Better World: Sydney Hilton Hotel, NSW, Australia, 18-21 September 2011, Barton, A.C.T.: Engineers Australia, 2011, pp. 1648-1660.
- [2] S. Porada, R. Zhao, A. van der Wal, V. Presser, P.M. Biesheuvel, "Review on the science and technology of water desalination by capacitive deionization", *Progress in Materials Science*, 58, 2013, pp. 1388-1442.
- [3] Li H, Pan L, Lu T, Zhan Y, Nie C, Sun Z., "A comparative study on electrosorptive behavior of carbon nanotubes and grapheme for capacitive deionization", *J Electroanal Chem.*, 2011, 653:40-4.
- [4] Oren Y., "Capacitive deionization for desalination and water treatment – past, present and future", *Desalination*, 2008, 228 (1-3), pp. 10-29.
- [5] <http://www.un.org/News/Press/docs/2010/ga10967.doc.htm>.
- [6] Anderson, M. A., Cudero, A. L., Palma, J., "Capacitive deionization as an electrochemical means of saving energy and delivering clean water. Comparison to present desalination practices: Will it compete?" *Electrochimica Acta.*, 2010, 55, pp. 3845-3856.
- [7] Xu, P., Drewes, J.E., Heil, D., Wang, G., "Treatment of brackish produced water using carbon aerogel based capacitive deionization technology", *Water Research*, 2008, 42, pp. 2605-2617.
- [8] Seo, S. J., Jeon, H., Lee, J. K., Kim, G. Y., Park, D., Nojima, H., Lee, J., Moon, S. H., "Investigation on removal of hardness ions by capacitive deionization (CDI) for water softening applications", *Water Research*, 2010, 44, pp. 2267-2275.
- [9] Broséus, R., Cigana, J., Barbeau, B., Daines-Martinez, C., Suty, H., "Removal of total dissolved solids, nitrates and ammonium ions from drinking water using chargebarrier capacitive deionization", *Desalination*, 2009, 249, pp. 217-223.
- [10] Ryoo MW, Kim JH, Seo G., "Role of titania incorporated on activated carbon cloth for capacitive deionization of NaCl solution", *J. Colloid Interface Sci.* 2003, 264 (2): 414-19.

- [11] Zhao R, Biesheuvel PM, Van der Wal A., "Energy consumption and constant current operation in membrane capacitive Deionization", *Energy Environ Sci*, 2012, 5:9520–7.
- [12] Demirer ON, Naylor RM, Rios Perez CA, Wilkes E, Hidrovo C., "Energetic performance optimization of a capacitive deionization system operating with transient cycles and brackish water", *Desalination* 2013,314:130–8.
- [13] Rica RA, Ziano R, Salerno D, Mantegazza F, Bazant MZ, Brogioli D., "Electro-diffusion of ions in porous electrodes for capacitive extraction of renewable energy from salinity differences", *Electrochim Acta*, 2013,92:304–14.
- [14] Kim Y-J, Choi J-H., "Improvement of desalination efficiency in capacitive deionization using a carbon electrode coated with an ion-exchange polymer", *Water Res*, 2010, 44:990–6.
- [15] Al-Zoubi, H., Hilal, N., Darwish, N.A., Mohammad, A.W., "Rejection and modelling of sulphate and potassium salts by nanofiltration membranes neural network and Spiegler-Kedem model", 2007, *Desalination*, 206, pp. 42-60.
- [16] M. Khayet, C. Cojocar, M. Essalhi, "Artificial neural network modeling and response surface methodology of desalination by reverse osmosis", *Journal of Membrane Science*, Volume 368, Issues 1–2, 15 February 2011, Pages 202–214.
- [17] R. Porrizzo, A. Cipollina, M. Galluzzo, G. Micale, "A neural network-based optimizing control system for a seawater-desalination solar-powered membrane distillation unit", *Computers & Chemical Engineering*, Volume 54, 11 July 2013, Pages 79–96.
- [18] Zhao, Y., Wang, Y., Wang, R., Wu, Y., Xu, S., Wang, J., "Performance comparison and energy consumption analysis of capacitive deionization and membrane capacitive deionization processes", *Desalination*, Volume 324, issue (September 2, 2013), pp. 127-133.
- [19] Shokoufe Tayyebi, Maryam Alishiri, "The control of MSF desalination plants based on inverse model control by neural network", *Desalination*, Volume 333, Issue 1, 15 January 2014, pp. 92–100.
- [20] Wang, H. J., Xi, X. K., Kleinhammes, A., Wu, Y., "Temperature-induced hydrophobic-hydrophilic transition observed by water adsorption", *Science*, 2008, 322, pp. 80-83.
- [21] Li, H., Zou, L., Pan, L., Sun, Z., "Using graphene nanoflakes as electrodes to remove ferric ions by capacitive deionization", *Separation and Purification Technology*, 2010, 75, pp. 8-14.
- [22] Adel El Shahat, "PV Module Optimum Operation Modeling", *Journal of Power Technologies*, Vol 94, No 1 (2014).
- [23] Adel El Shahat, "PM Synchronous Machine New Aspects; Modeling, control, and design", ISBN 978-3-659-25359-1, LAP Lambert Academic Publishing, Germany, 2012.
- [24] Adel El Shahat, "DC-DC Converter Duty Cycle ANN Estimation for DG Applications", *Journal of Electrical Systems (JES)*, ISSN 1112-5209; Vol. 9, Issue 1, March 2013.
- [25] Adel El Shahat, and Hamed El Shewy, "High Fundamental Frequency PM Synchronous Motor Design Neural Regression Function", *Journal of Electrical Engineering*, ISSN 1582-4594; Article 10.1.14, Edition 1, March, Vol. 10 / 2010.
- [26] A. El Shahat, and H. El Shewy, "PM Synchronous Motor Control Strategies with Their Neural Network Regression Functions", *Journal of Electrical Systems (JES)*, ISSN 1112-5209; Vol. 5, Issue 4, Dec. 2009.
- [27] Adel El Shahat, "Photovoltaic Power System Simulation for Micro – Grid Distribution Generation", 8th International Conference on Electrical Engineering, 29-31 May, 2012, Military Technical College, Egypt; EE137, ICEENG 2012.
- [28] A. El Shahat, H. El Shewy, "Neural Unit for PM Synchronous Machine Performance Improvement used for Renewable Energy", Paper Ref.: 910, Global Conference on Renewable and Energy Efficiency for Desert Regions (GCREEDER2009), Amman, Jordan.
- [29] Adel El Shahat, "PV Cell Module Modeling & ANN Simulation for Smart Grid Applications", *Journal of Theoretical and Applied Information Technology*, E-ISSN 1817-3195; ISSN 1992-8645; Vol. 16, No.1, June 2010, pp. 9 – 20.

**Dr. Adel El Shahat** is currently a Visiting Assistant Professor, Department of Electrical and Computer Engineering at University of Illinois, Chicago (UIC), Laboratory for Energy and Switching-Electronics Systems (LESES) (2014:Present). Assistant Professor in Engineering Science Department, Faculty of Petroleum and Mining Engineering, Suez University, Egypt (2011:2014). Previously, he was Visiting Researcher, ECE Dept., Mechatronics-Green Energy Lab, The Ohio State University, USA (2008: Sept.2010). His interests are: Photovoltaic power, Wind Energy, Electric Machines, Artificial Intelligence, Renewable Energy, Power System, Control Systems, Power Electronics, and Smart Grids. He was Associate Lecturer (2004:2008) in Faculty of Petroleum & Mining Engineering, Suez Canal University, Egypt, and Teaching Assistant (2000:2004) in the same faculty. His Education: PhD in Electrical Engineering (2011), Through Joint Supervision between Ohio State University, USA and Zagazig University, Egypt; M.Sc. in Electrical Engineering 2004, and B.Sc. in Electrical Engineering 1999 from Faculty of Engineering, Zagazig University. He has many publications between international Journals papers, refereed conferences papers, books, book chapters and abstracts or posters. He is a Member of IEEE, IEEE Computer Society, ASEE, IAENG, IACSIT, EES, WASET and ARISE. Also, he is member of editorial team and reviewer for six international journals. He gains honors and recognitions from The Ohio State University, USA 2009, Suez Canal University Honor with university Medal in 2012, 2006, Merit Ten Top-up Students Award of each Faculty from Arab Republic of Egypt, in 2000, and EES, 1999, Egypt, and also student distinguished awards (1994:1999) from Helwan, and Zagazig University, Egypt.